International Journal of Nanoelectronics and Materials
IJNeaM
ISSN 1985-5761 | E-ISSN 2232-1535

# Upcycling face mask waste into activated carbon: Synthesis and characterization via chemical activation

Nur Amaliyana Raship [a], Muhammad Amirudin Abdul Rahman [b], and Siti Nooraya Mohd Tawil [a,b] *

[a]*Centre for Tropicalisation, Defence Research Institute, Universiti Pertahanan Nasional Malaysia (UPNM), Kem Sungai Besi 57000, Kuala Lumpur, Malaysia*
[b]*Department of Electrical and Electronic Engineering, Faculty of Engineering, Universiti Pertahanan Nasional Malaysia (UPNM), Kem Sungai Besi 57000, Kuala Lumpur, Malaysia*
** Corresponding author. e-mail: nooraya@upnm.edu.my*

Received 13 March 2025, Revised 3 November 2025, Accepted 24 November 2025

**ABSTRACT**

This study reports the synthesis and characterization of activated carbon (AC) derived from face mask waste using chemical activation subsequent carbonization at temperatures varied between 650–850°C. The structural, morphological, and electrical properties of the resulting AC were probed using Fourier-transform infrared spectroscopy (FTIR), Raman spectroscopy, field emission scanning electron microscopy (FESEM), energy-dispersive X-ray spectroscopy (EDS), and electrical potential measurement of the AC electrode. The findings show that the structural, morphological, and electrical characteristics of the AC are strongly influenced by the carbonization temperature. The existence of functional groups-graphitic carbon, and carbonaceous materials was demonstrated by FTIR and Raman studies, respectively. The sample carbonized at 650°C exhibited the highest degree of disorder, a fibrous porous structure, and the greatest carbon content. Notably, this sample demonstrated the highest voltage output (35 mV) when employed as an electrode in a supercapacitor, indicating superior energy storage capability. This study emphasizes the potential of converting face mask waste into functional AC for sustainable energy storage applications, specifically supercapacitors.

**Keywords:** *Face mask waste, Activated carbon, Carbonization, Chemical activation, AC electrode; Supercapacitors*

## 1. INTRODUCTION

With the global spread of the COVID-19 pandemic, disposable face masks have become essential in people's daily life. This has led to a dramatic increase in face mask usage around the world, generating massive volumes of face mask waste and contributing to environmental issues. As stated in data published by Sangkham *et al.* [1], monthly use of face masks in Asia has dramatically risen to 2,228,170,832 in 2020. Similarly, Torres *et al.* [2] reported that nearly three million face masks are discarded globally every minute. In conjunction, a tremendous quantity of contaminated face mask waste is improperly disposed of in public areas such as parking lots, hospitals, and streets, posing threats to public health and the environment [3]. Traditionally, face mask waste has been treated similarly to ordinary polymer waste, primarily through direct landfilling or incineration [4]. However, this traditional method is limited by the resource efficiency and the risk of secondary pollution issues, including the release of microplastics, plasticizers, heavy metals, plasticizer synthetic antioxidants [5]. Therefore, the development of innovative recycling approaches to convert face mask waste into high-value materials is crucial for both resource recovery and waste management.

Until now, there has been a growing focus on alternative methods of transforming face mask waste into valuable carbon-based materials [6–8], fine chemicals [9], and fuels [10–12]. Since face masks are mainly composed of polypropylene (PP), which contains over 85% carbon [13], researchers have explored the transformation of PP into functional carbon materials such as graphene [14], carbon nanotubes (CNTs) [15–17], carbon nanosheets [18], and activated carbon (AC) [19, 20]. Previously, several studies have reported synthesizing carbon-based materials using physical activation [7, 8], chemical activation [20, 21], and other physicochemical activation, including hydrothermal [22], catalytic [23], and microwave heating [24]. Thus, recycling face mask waste into carbon-based materials not only mitigates pollution but also provides a cost-effective alternative to traditional carbon sources. In addition, production of carbon-based materials from face mask waste has potential applications in a variety of fields, including sustainable environmental ($CO_2$) capture [25] and green energy storage (supercapacitors [26, 27], batteries [28]). This is owing to their excellent electrochemical performance, high conductivity, and large surface area [19, 20]. Therefore, recycling face mask waste into carbon-based products is crucial to reducing environmental pollution and offering a reasonably priced substitute for traditional carbon sources.

In this study, we investigate the chemical activation method for producing AC from face mask waste. By optimizing synthesis parameters, we aim to obtain AC with high carbon yield, a good degree of disorder, good morphology with high porosity and large specific surface area, high electrical

conductivity, and strong stability. Furthermore, we examine the effects of activating agents and carbonization temperatures on the structural and morphological properties of the resulting material. Finally, the potential application of the produced AC as an electrode material is evaluated through the assembly of supercapacitors.

## 2. EXPERIMENTAL DETAILS

### 2.1. Materials Preparation

Firstly, the waste from face masks was cut and manually separated into its components: wire, ear strap, middle layer, outer layer, and nose strip. Only the outer and inner were used for the synthesis process. These layers were cut into small pieces and weighed to approximately 30 g using a precision scale (Mettler Toledo). For chemical activation, 30 g of the mask pieces were immersed in 100 mL of 1M potassium hydroxide (KOH) solution (Merck, Germany) for 1 hour. After immersion, the samples were dried in an oven at 105°C for 1 hour to remove the moisture. After the drying process, the samples were placed into a crucible and carbonized for 1 hour in a furnace at ambient atmospheric conditions. The carbonization temperatures were varied at 650°C, 750°C, and 850°C. The resulting AC samples were labeled as AC-650°C, AC-750°C, and AC-850°C. Finally, the sample was rinsed with distilled water and sulfuric acid until the pH level reached 7. The experimental process of AC is illustrated in Figure 1.

### 2.2. Materials Characterization

A range of characterization methods, including Fourier-transform infrared spectroscopy (FTIR), Raman spectroscopy, field emission scanning electron microscopy (FESEM), and energy-dispersive X-ray spectroscopy (EDS), were employed to evaluate the properties of the AC derived from outer and inner layers of face mask waste. FTIR (Perkin Elmer, model: Frontier) with mode KBR pellets was used to identify the functional groups of polypropylene (PP) materials from face mask waste and AC powder. RAMAN (model: Renishaw) was used to determine the structural characteristics, with a laser wavelength of 532 nm, a range of Raman shift between 500 $cm^{-1}$ and 3000 $cm^{-1,}$ and a laser power of 10%. The details of surface morphology were assessed using FESEM (model: ZEISS), while the AC composition was measured using FESEM equipped with energy dispersive X-ray (EDS).

### 2.3. Electrical Potential Measurements of the AC electrode

Initially, the aluminum foils were cut into 11 cm × 15 cm dimensions. The surfaces of the aluminum foils were then polished with sandpaper to enhance conductivity. Subsequently, a slurry paste was produced by combining the AC, a KOH solution, and white glue, which was then applied to the aluminum foil surfaces. The slurry paste was formulated using AC obtained at AC-650°C, AC-750°C, and AC-850°C. The AC-coated electrodes were dried at room temperature for 3 hours. Next, the AC supercapacitor was assembled using an AC electrode as both the cathode and anode with a layer of paper serving as the membrane in a KOH electrolyte. The AC supercapacitor was then charged using a battery charger (UltraPower; UP200 Duo AC/DC charger), and a multimeter was used to measure the electrical potential of the AC supercapacitors. The schematic diagram of an AC supercapacitor is illustrated in Figure 2.

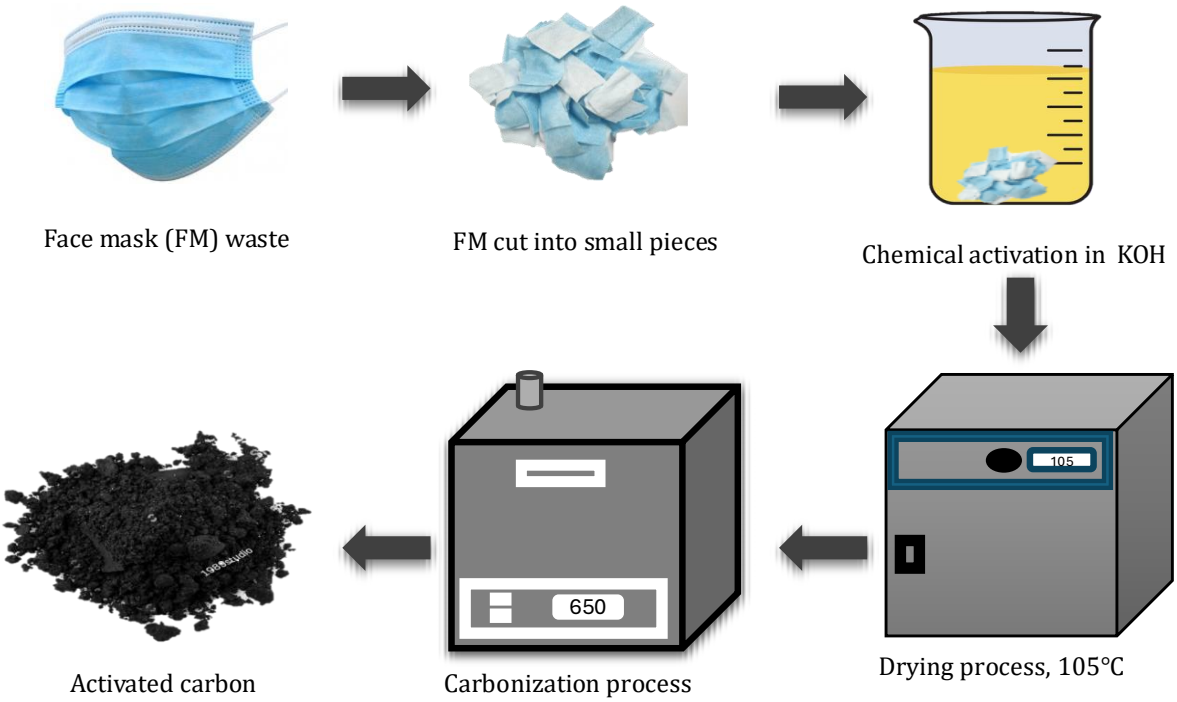


**Figure 1**. Synthesis process of activated carbon

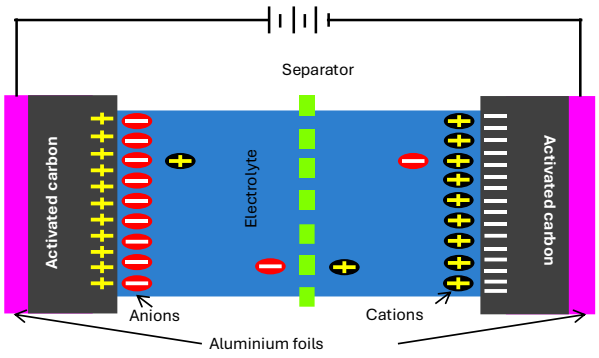


**Figure 2**. The schematic diagram of an AC supercapacitor

## 3. RESULTS AND DISCUSSION

### 3.1. Characterization of Face Mask Waste

Prior to upcycling the face mask waste AC, it is essential to analyze the material properties and structure to confirm its composition. This is to verify that the material of the face mask is made up of polypropylene (PP) materials. According to Yuwen *et al.* [6], PP materials make up a large portion of face mask waste, with a carbon content as high as 79.37%. Thus, utilizing face mask waste as a carbon precursor for producing high-value AC presents a viable recycling approach and holds promise for energy storage applications. Figure 3 displays the FTIR spectra of various face mask components, including the nose strip, inner layer, outer layer, and middle layer.

In all components of the dissembled face masks waste, characteristics were observed near 1377 $cm^{-1}$ and 1455 $cm^{-1}$ corresponding to $CH_2$ bending and $CH_3$ bending vibrations, respectively. Additionally, a peak around 2917 $cm^{-1}$, attributed to C–H stretching, was also identified. All the peaks exhibit the characteristic FTIR peak of polypropylene, confirming that the face mask waste is primarily composed of PP. These results are comparable with findings reported by Yuwen *et al.* [6] and Jung *et al.* [29].

### 3.2. Effect of Activating Agent

Two synthesis approaches were used to determine the effectiveness of chemical activation in increasing carbon yield and improving the characteristics of the resulting AC. In the first approach, the FM sample was immersed in a KOH activating agent prior to undergoing the carbonization process. While the second approach involved direct carbonization of the FM waste without the use of any activating agent. Figure 4 presents the FTIR spectra of the carbon materials synthesized with and without the activating agent of KOH. The FTIR spectra exhibited significant absorption bands around 3400 $cm^{-1}$, corresponding to O–H stretching vibrations, suggesting the existence of hydroxyl groups. Notably, these peaks were more prominent in the KOH-activated samples, suggesting that chemical activation improved surface functionality of the carbon materials. A characteristics peaks near 1642 $cm^{-1}$, attributed to C=O stretching was also stronger in the chemically activated samples, indicating a higher degree of graphitization and a more developed polyaromatic carbon structure [24]. These support the notion that chemical activation with KOH can increase the carbon yield during carbonization [30]. Additionally, a peak at 1442 $cm^{-1}$, referring to symmetric bending of $-CH_2$ groups, was observed and is attributed to the residual PP chains. Peaks observed near 1118 $cm^{-1}$, and 1022 $cm^{-1}$ corresponding to O=S=O stretching vibration, which refers to sulfonyl group [31]. These features are likely a result of the rinsing process with sulfuric acid during sample preparation.

The yield percentage (%) of AC derived from face mask waste was determined using the following formula (Equation (1)), in order to assess the efficiency of chemical activation in enhancing the carbon yield:

$$\text{Yield } \% = \frac{\text{Final weight of AC (g)}}{\text{Initial weight of AC (g)}} \times 100 \quad (1)$$

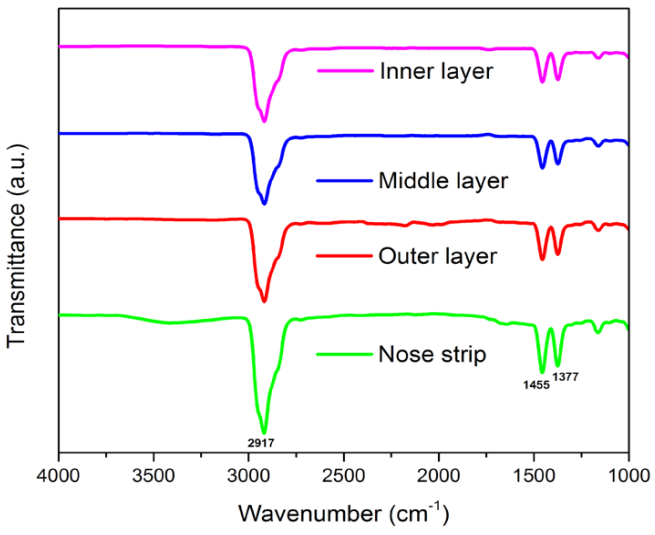


**Figure 3**. FTIR spectra of different components in face mask waste

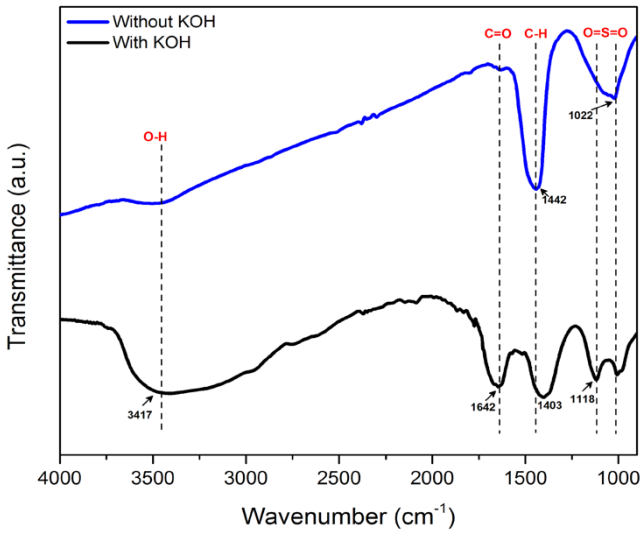


**Figure 4**. FTIR spectra of carbon materials with KOH in comparison to without KOH

Table 1 shows the amount of carbon yield for samples prepared with and without KOH activation. Based on the calculation, a sample that immersed in KOH exhibited a high carbon yield of 13.3%. Thus, this confirms that the synthesis of AC through a combination of chemical activation and carbonization process improves the overall carbon yield. Tajer *et al.* [32] and Chukwu *et al.* [33], who observed that chemical activation using agents such as KOH is more effective in achieving higher carbon yields compared to physical activation alone.

### 3.3. Effect of Carbonization Temperature

The FTIR spectra shown in Figure 5 were obtained to validate the surface functional group of activated carbon at various carbonization temperatures. Peaks found between 3400 $cm^{-1}$ and 3551 $cm^{-1}$ correspond to O–H stretching vibrations, indicating the presence of hydroxyl groups [9]. The peaks detected at 1424 $cm^{-1}$, 2873 $cm^{-1}$, and 2961 $cm^{-1}$ reflect symmetric bending, asymmetric stretching, and symmetric stretching of $-CH_2$ groups, respectively, suggesting the presence of residual PP [28]. A minor peak appears at 1799 $cm^{-1}$, attributed to C=O stretching vibrations [34], indicating the presence of carbonyl groups, which contribute to the charge storage capability [34]. Notably, the C=O peak was more pronounced in the AC-650°C sample, suggesting enhanced potential for charge storage. Additionally, a peak at 1622 $cm^{-1}$ corresponds to C=C stretching vibrations, indicative of aromatic structures, indicating the characteristics of graphitic carbon [35]. This peak was more prominent in the AC-850°C sample, indicating a higher graphitization. A peak around 1137 $cm^{-1}$, attributed to O=S=O stretching, indicates the presence of sulfonyl groups, which is caused by the rinse procedure with sulfuric acid during sample preparation. Overall, the AC-650°C sample develops more structural defects and functional groups that can serve as active sites for charge storage, thereby improving the electrical performance of the supercapacitor.

The structural evolution of AC at various carbonization temperatures was further investigated using Raman spectroscopy, as demonstrated in Figure 6. Broad Raman bands were detected around 1350 $cm^{-1}$ and 1580 $cm^{-1}$, corresponding to the D band and G band, respectively, for all samples. The D band is associated with disordered carbon structures, while the G band corresponds to the graphitic structure of carbon, indicating the formation of a highly amorphous carbon-like structure [9, 19]. The Raman spectrum for the AC-650°C sample exhibited strong and narrow peaks for both D and G bands. In the AC-750°C sample, the D band intensity decreased relatively to the G band, suggesting improved graphitization. However, at 850°C, a significant reduction in the intensity of both D and G bands was observed compared to the AC-650°C sample, indicating structural changes at higher temperature. The difference in the intensity of both the D band and G band was examined to determine the degree of disorder in AC. The following formula in Equation (2) can be used to calculate the ratio of the intensity of these bands:

$$\text{Degree of disorder} = \frac{I_D}{I_G} = \frac{\text{Intensity of D band}}{\text{Intensity of G band}} \quad (2)$$

Based on the calculations, the disorder degree of AC-650°C, AC-750°C, and AC-850°C were 0.45, 0.43, and 0.33, respectively. The disorder degree of the samples decreased with the increase of carbonization temperature. Note that the decreased intensity ratio of D/G bands implies a greater graphitization degree with low structural disorder [8]. This structural disorder is consistent with the presence of functional groups observed in the FTIR spectra. Additionally, this finding implies that the AC-650°C sample may possess more defect sites, which may lead to an increase in the concentration of adsorption-active sites [24]. These defects are expected to increase the ability of AC

**Table 1.** Carbon yield (%) of activated carbon

| Sample | Initial weight of face mask (g) | Final weight of AC (g) | Carbon yield (%) |
|---|---|---|---|
| With KOH | 20.0 | 2.6654 | 13.3 |
| Without KOH | 20.0 | 0.1212 | 0.6 |

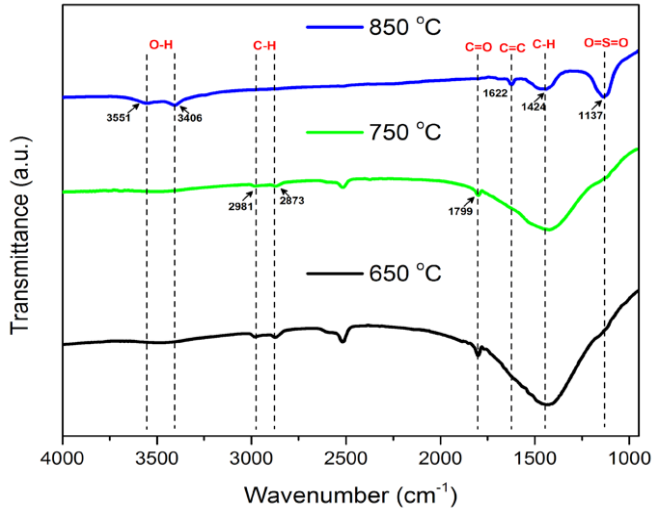


**Figure 5**. FTIR spectra of AC at various carbonization temperatures

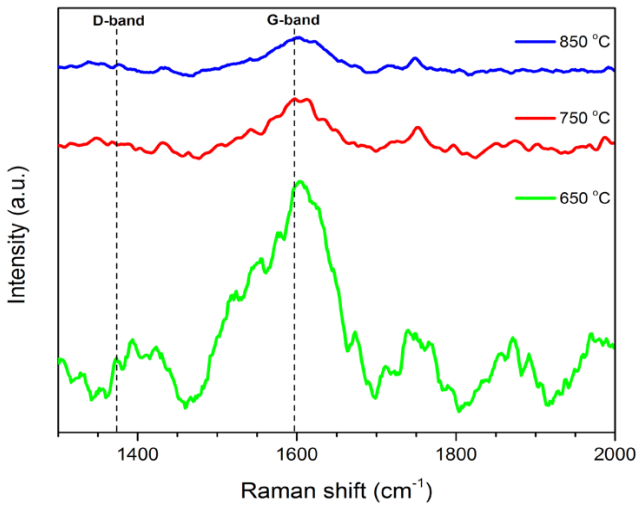


**Figure 6**. RAMAN spectra of AC at various carbonization temperatures

to store charge and may play a role in improving the electrical potential performance of the supercapacitor.

The FESEM images in Figure 7 present the surface morphology of activated carbon carbonized at 650°C, 750°C, and 850°C. Each sample was examined at two different magnifications, which Figures 7 (a), (c), (e) display 1000× magnifications and Figure 7 (b), (d), (f) displays 10,000× magnifications. As shown in the images, the fibrous structure of the carbon material gradually breaks down into agglomerated and dense forms with increasing carbonization temperature. FESEM images of the AC-650°C sample were shown in Figure 7 (a–b), revealing a well-defined fibrous morphology with numerous tiny pores. This porous structure, along with high surface area, provides large active sites and is effective in ion transport [18]. The visible fibers suggest that the original fibrous structure of the face mask waste is conserved during the carbonization process at this temperature. In contrast, the morphology of the AC-750°C sample shown in Figure 7 (c–d) displays significant compaction and aggregation, with less apparent fibrous features compared to the AC-650°C sample. Further increase in the carbonization temperature to 850°C (Figure 7 (e–f)), the morphology exhibits a very compact structure with fewer visible pores and a largely broken-down fiber structure. This indicates that the carbonization process at 850°C results in extensive graphitization and loss of the original fibrous morphology. According to Hu *et al.* [22], the fibrous structure of masks material begins to degrade at a temperature above 430°C, and the carbonization temperature of 850°C exceeds the thermal decomposition point of the PP polymer chain. These morphological transitions align with Raman and FTIR studies, where higher carbonization temperatures lead to fewer functional groups, increased graphitization, and a decrease in structural disorder. Ultimately, the preservation of fibrous structure and the high surface area observed in the AC-650°C sample could manifest the potential as an effective electrode material for supercapacitor applications.

The EDS analysis was conducted to determine the elemental composition of the activated carbon. Table 2 shows the weight percentage (wt%) of elements in AC carbonized at 650°C, 750°C, and 850°C, which are mainly composed of carbon and oxygen elements. The results reveal a clear trend: as carbonization temperatures increase, the carbon content decreases while the oxygen content increases. Specifically, the AC-650°C sample exhibits the highest carbon content with nearly a balanced ratio of carbon to oxygen. The high carbon content indicates that a significant portion of the original carbon structure is retained, which corresponds with the well-preserved fibrous morphology observed in the FESEM images. As the carbonization temperature increases to 750°C and 850°C, a notable reduction in carbon content is observed, accompanied by an increase in oxygen content. This high oxygen content indicates the existence of a substantial number of oxygen-containing functional groups preserved during high carbonization temperature [31]. These oxygen functional groups can promote the cross-linking of PP molecules and inhibit the rearrangement of the microcrystalline structure, thereby enhancing the interlayer dispersion within the carbon material [36–37]. This trend is consistent with the observations from FTIR, Raman, and FESEM analysis.

**Table 2.** Weight percentage (wt%) of activated carbon at various carbonization temperatures

| Sample | Initial weight of face mask (g) | Final weight of AC (g) |
|---|---|---|
| AC-650°C | 49.43 | 50.57 |
| AC-750°C | 31.66 | 68.34 |
| AC-850°C | 27.01 | 72.99 |

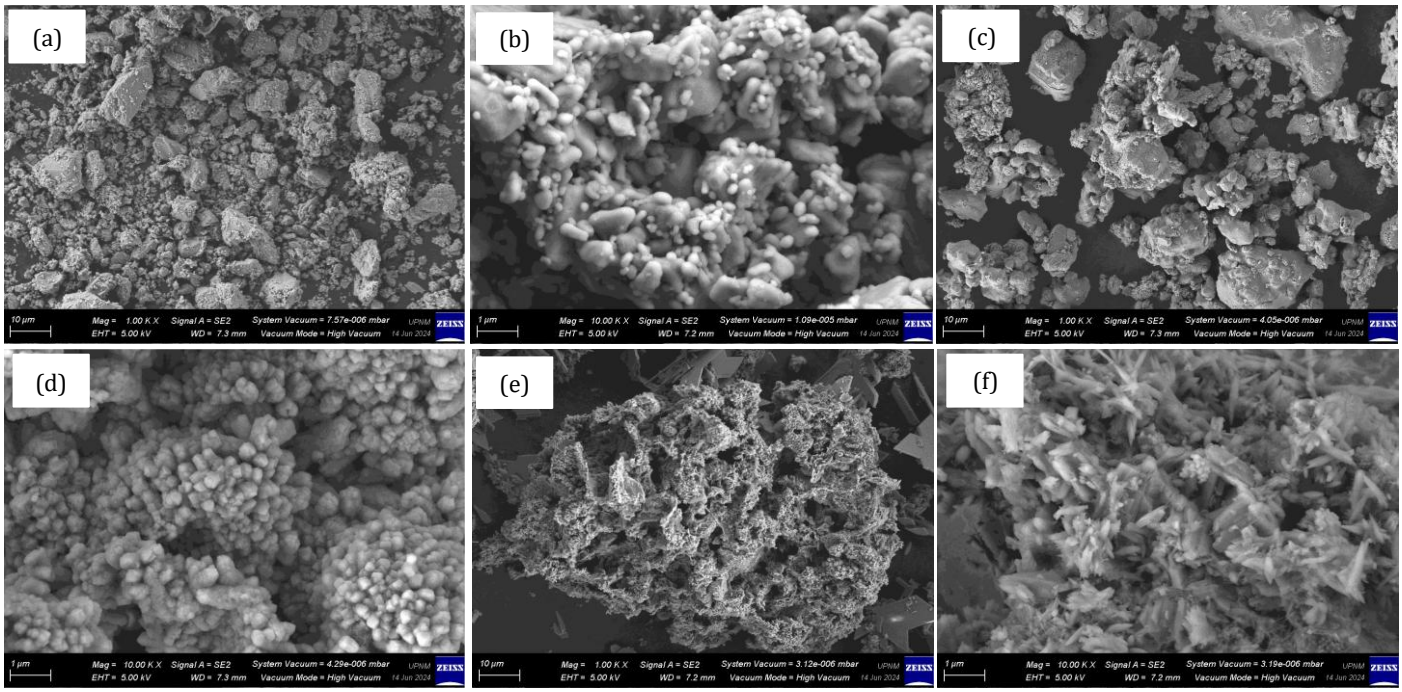


**Figure 7**. FESEM images of AC at various carbonization temperatures (a–b) 650°C (c–d) 750°C, and (e–f) 850°C

Overall, the higher carbon content and balanced oxygen composition of the AC-650°C sample could ensure good electrical conductivity and surface characteristics, making it a promising candidate for high-performance supercapacitor applications.

To assess the electrical potential of AC for supercapacitor applications, a basic supercapacitor was fabricated using AC as both the anode and cathode in a KOH electrolyte. The electrical performance of the supercapacitors was tabulated in Table 3, which provides insights into the practical demonstration of energy storage of the AC electrodes. The measured voltage values for supercapacitors using AC-650°C, AC-750°C, and AC-850°C samples were 35 mV, 25 mV, and 22 mV, respectively. Among the samples, the AC-650°C sample achieved the highest voltage value, indicating superior energy storage potential. This enhanced performance can be attributed to its fibrous structure, numerous functional groups, high disorder degree, and well-balanced elemental composition. In contrast, samples carbonized at higher temperatures exhibit lower voltage output due to their compact morphological structure, fewer functional groups, and increased oxidation levels. Considering these factors, the AC carbonized at 650°C shows exceptional characteristics for supercapacitor electrodes and benefits towards energy storage applications.

**Table 3.** Electrical performance of the AC electrode for the supercapacitor

| Sample | Voltage (mV) |
|---|---|
| AC-650°C | 35 |
| AC-750°C | 25 |
| AC-850°C | 22 |

## 4. CONCLUSIONS

In summary, activated carbon (AC) was successfully synthesized from face mask waste using a combined chemical activation-carbonization method. Chemical activation using KOH solution effectively enhanced the functional groups of polypropylene (PP) and significantly enhanced the carbon yield. The combination of chemical activation and carbonization at various temperatures was found to strongly influence the structural, morphological, and electrical properties of the resulting activated carbon derived from face mask waste. FTIR analysis reveals the presence of various functional groups, while Raman spectroscopy reveals a high degree of disorder in the AC produced at 650°C. FESEM images demonstrate that the AC-650°C sample has a fibrous morphology with numerous micro-pores, offering a large surface area conducive to ion adsorption and charge storage. EDS analysis confirmed the composition of only carbon and oxygen elements, with AC-650°C exhibiting a well a balance carbon to -oxygen ratio. As a consequence, the supercapacitor fabricated with AC-650°C achieved the highest voltage output value of 35 mV, indicating superior energy storage capability. These results highlight the significance of controlling carbonization conditions to improve the properties as well as performance of activated carbon electrodes towards sustainable energy storage applications.

## ACKNOWLEDGMENTS

This research was supported by a grant from FRGS/1/2023/TK08/UPNM/02/3. This research is also funded by Grant UPNM/2024/GPPP/TK/1 from Universiti Pertahanan Nasional Malaysia.

## REFERENCES

[1] S. Sangkham, "Face mask and medical waste disposal during the novel COVID-19 pandemic in Asia," *Case Studies in Chemical and Environmental Engineering*, vol. 2, p. 100052, 2020.

[2] F. G. Torres and G. E. De-la-Torre, "Face mask waste generation and management during the COVID-19 pandemic: An overview and the Peruvian case," *Science of The Total Environment*, vol. 786, p. 147628, 2021.

[3] C. Nzediegwu and S. X. Chang, "Improper solid waste management increases potential for COVID-19 spread in developing countries," *Resources, Conservation and Recycling*, vol. 161, p. 104947, 2020.

[4] S. Akhtar, K. Pranay, and K. Kumari, "Personal protective equipment and micro-nano plastics: A review of an unavoidable interrelation for a global well-being hazard," *Hygiene and Environmental Health Advances*, vol. 6, p. 100055, 2023.

[5] S. S. Ray, H. K. Lee, D. T. T. Huyen, S.-S. Chen, and Y.-N. Kwon, "Microplastics waste in environment: A perspective on recycling issues from PPE kits and face masks during the COVID-19 pandemic," *Environmental Technology & Innovation*, vol. 26, p. 102290, 2022.

[6] C. Yuwen, B. Liu, Q. Rong, L. Zhang, and S. Guo, "Porous carbon materials derived from discarded COVID-19 masks via microwave solvothermal method for lithium-sulfur batteries," *Science of The Total Environment*, vol. 817, p. 152995, 2022.

[7] Q. Sun, T. Liu, T. Wen, and J. Yu, "Coupling of carbonization method with high-energy ball milling: Towards submicron-sized graphite powders transforming from waste COVID-19 masks," *Materials Chemistry and Physics*, vol. 307, p. 128134, 2023.

[8] Y. Gao *et al.*, "Recycling spent masks to fabricate flexible hard carbon anode toward advanced sodium energy storage," *Journal of Electroanalytical Chemistry*, vol. 941, p. 117525, 2023.

[9] H. Hao, F. Shen, J. Yang, M. Qiu, H. Guo, and X. Qi, "Synthesis of Sulfonated Carbon from Discarded Masks for Effective Production of 5-Hydroxymethylfurfural," *Catalysts*, vol. 12, no. 12, p. 1567, 2022.

[10] S. Yousef, J. Eimontas, N. Striūgas, and M. A. Abdelnaby, "A new strategy for butanol extraction from COVID-19 mask using catalytic pyrolysis process over ZSM-5 zeolite catalyst and its kinetic behavior," *Thermochimica Acta*, vol. 711, p. 179198, 2022.

[11] Y. Jiang, R. Xu, C. Zeng, K. Wang, L. Han, and X. Zhang, "Scalable decomposition-catalysis of disposable

COVID-19 face mask over self-assembly metal-doping carbocatalysts for tunable value-added products," *Applied Catalysis B: Environmental*, vol. 317, p. 121735, 2022.

[12] J. Wang, J. Jiang, Y. Zhang, X. Meng, and A. J. Ragauskas, "Upcycling disposable face masks into fuel range iso-alkanes through hydropyrolysis coupled with vapor-phase hydrocracking," *Energy*, vol. 263, p. 125843, 2023.

[13] L. Lyu *et al.*, "Towards environmentally sustainable management: A review on the generation, degradation, and recycling of polypropylene face mask waste," *Journal of Hazardous Materials*, vol. 461, p. 132566, 2024.

[14] A. B. Irez, C. Okan, R. Kaya, and E. Cebe, "Development of recycled disposable mask based polypropylene matrix composites: Microwave self-healing via graphene nanoplatelets," *Sustainable Materials and Technologies*, vol. 31, p. e00389, 2022.

[15] W. Yang, L. Cao, W. Li, X. Du, Z. Lin, and P. Zhang, "Carbon Nanotube prepared by catalytic pyrolysis as the electrode for supercapacitors from polypropylene wasted face masks," *Ionics*, vol. 28, no. 7, pp. 3489–3500, 2022.

[16] R. Yu *et al.*, "A green and high-yield route to recycle waste masks into CNTs/Ni hybrids via catalytic carbonization and their application for superior microwave absorption," *Applied Catalysis B: Environmental*, vol. 298, p. 120544, 2021.

[17] V. S. Gangoli, T. Mahy, T. Yick, Y. Niu, R. E. Palmer, and A. Orbaek White, "Upcycling of face masks to application-rich multi- and single-walled carbon nanotubes," *Carbon Letters*, vol. 32, no. 7, pp. 1681–1688, 2022.

[18] X. Liu *et al.*, "Highly efficient conversion of waste plastic into thin carbon nanosheets for superior capacitive energy storage," *Carbon*, vol. 171, pp. 819–828, 2021.

[19] Z. Zhu *et al.*, "Synthesis of the cathode and anode materials from discarded surgical masks for high-performance asymmetric supercapacitors," *Journal of Colloid and Interface Science*, vol. 603, pp. 157–164, 2021.

[20] J. Sreńscek-Nazzal, J. Serafin, A. Kamińska, A. Dymerska, E. Mijowska, and B. Michalkiewicz, "Waste-based nanoarchitectonics with face masks as valuable starting material for high-performance supercapacitors," *Journal of Colloid and Interface Science*, vol. 627, pp. 978–991, 2022.

[21] A. Ahmed, S. Verma, P. Mahajan, A. K. Sundramoorthy, and S. Arya, "Upcycling of surgical facemasks into carbon based thin film electrode for supercapacitor technology," *Scientific Reports*, vol. 13, no. 1, p. 12146, 2023.

[22] X. Hu and Z. Lin, "Transforming waste polypropylene face masks into S-doped porous carbon as the cathode electrode for supercapacitors," *Ionics*, vol. 27, no. 5, pp. 2169–2179, 2021.

[23] J. Zhang *et al.*, "Resource utilization of waste masks in simultaneous high efficient removal of Light Green SF and Cr(VI) via microwave catalytic technology," *Separation and Purification Technology*, vol. 330, p. 125523, 2024.

[24] C. Yuwen, B. Liu, Q. Rong, L. Zhang, and S. Guo, "Self-activated pyrolytic synthesis of S, N and O co-doped porous carbon derived from discarded COVID-19 masks for lithium sulfur batteries," *Renewable Energy*, vol. 192, pp. 58–66, 2022.

[25] J. Serafin, J. Sreńscek-Nazzal, A. Kamińska, O. Paszkiewicz, and B. Michalkiewicz, "Management of surgical mask waste to activated carbons for $CO_2$ capture," *Journal of $CO_2$ Utilization*, vol. 59, p. 101970, 2022.

[26] N. A. Raship, S. N. M. Tawil, and M. Syaripuddin, "PPE Waste-Derived Carbon Materials for Energy Storage Applications via Carbonization Techniques," *C*, vol. 11, no. 1, p. 8, 2025.

[27] R. Mendoza, J. Oliva, K. P. Padmasree, A. I. Oliva, A. I. Mtz-Enriquez, and A. Zakhidov, "Highly efficient textile supercapacitors made with face masks waste and thermoelectric $Ca_3Co_4O_{9-\delta}$ oxide," *Journal of Energy Storage*, vol. 46, p. 103818, 2022.

[28] G. Lee, M. Eui Lee, S.-S. Kim, H.-I. Joh, and S. Lee, "Efficient upcycling of polypropylene-based waste disposable masks into hard carbons for anodes in sodium ion batteries," *Journal of Industrial and Engineering Chemistry*, vol. 105, pp. 268–277, 2022.

[29] M. R. Jung *et al.*, "Validation of ATR FT-IR to identify polymers of plastic marine debris, including those ingested by marine organisms," *Marine Pollution Bulletin*, vol. 127, pp. 704–716, 2018.

[30] Z. Miao *et al.*, "High-Performance Symmetric Supercapacitor Constructed Using Carbon Cloth Boosted by Engineering Oxygen-Containing Functional Groups," *ACS Applied Materials & Interfaces*, vol. 11, no. 19, pp. 18044–18050, 2019.

[31] S. Zhang, N. Sun, M. Jiang, R. A. Soomro, and B. Xu, "Trash to treasure: Sulfonation-assisted transformation of waste masks into high-performance carbon anode for sodium-ion batteries," *Carbon*, vol. 209, p. 118034, 2023.

[32] M. Tajer, M. Anbia, and S. Salehi, "Fabrication of polyacrylonitrile hybrid nanofiber scaffold containing activated carbon by electrospinning process as nanofilter media for $SO_2$, $CO_2$, and $CH_4$ adsorption," *Environmental Progress & Sustainable Energy*, vol. 40, no. 1, 2021.

[33] M. M. Chukwu *et al.*, "Adsorptive Capacity of Coconut Fibre Carbon Activated by Potassium Hydroxide for Wastewater Treatment," *International Journal of Advanced Science and Engineering*, vol. 9, no. 2, pp. 2669–2677, 2022.

[34] S. Foorginezhad, M. M. Zerafat, M. Asadnia, and G. Rezvannasab, "Activated porous carbon derived from sawdust for $CO_2$ capture," *Materials Chemistry and Physics*, vol. 317, p. 129177, 2024.

[35] M. M. Harussani, S. M. Sapuan, U. Rashid, and A. Khalina, "Development and Characterization of Polypropylene Waste from Personal Protective Equipment (PPE)-Derived Char-Filled Sugar Palm Starch Biocomposite Briquettes," *Polymers*, vol. 13, no. 11, p. 1707, 2021.

[36] Y. Lu *et al.*, "Pre-Oxidation-Tuned Microstructures of Carbon Anodes Derived from Pitch for Enhancing Na Storage Performance," *Advanced Energy Materials*, vol. 8, no. 27, 2018.

[37] C. Chen *et al.*, "Nonignorable Influence of Oxygen in Hard Carbon for Sodium Ion Storage," *ACS Sustainable Chemistry & Engineering*, vol. 8, no. 3, pp. 1497–1506, 2020.